Symmetry-protected line nodes and Majorana flat bands in nodal crystalline superconductors

Shingo Kobayashi, Shuntaro Sumita, Youichi Yanase, and Masatoshi Sato

Phys. Rev. B **97**, 180504 — Published 11 May 2018

DOI: 10.1103/PhysRevB.97.180504

Symmetry-protected line nodes and Majorana flat bands in nodal crystalline superconductors

Shingo Kobayashi,[1,2] Shuntaro Sumita,[3] Youichi Yanase,[3] and Masatoshi Sato[4]

[1] *Institute for Advanced Research, Nagoya University, Nagoya 464-8601, Japan*
[2] *Department of Applied Physics, Nagoya University, Nagoya 464-8603, Japan*
[3] *Department of Physics, Kyoto University, Kyoto 606-8502, Japan*
[4] *Yukawa Institute for Theoretical Physics, Kyoto University, Kyoto 606-8502, Japan*

(Dated: April 30, 2018)

Line nodes in the superconducting gap are known to be a source of Majorana flat bands (MFBs) on a surface. Here, we extend this relation to all symmetry-protected line nodes where an additional constraint arising from crystal symmetry destabilizes or hides the existence of MFBs. By establishing a one-to-one correspondence between group theoretical and topological classifications, we are able to classify the possible line-node-induced MFBs, including cases with (magnetic) non-symmorphic space groups. Our theoretical analysis reveals MFBs in antiferromagnetic superconductors.

Over the last few years, the study of nodal gap structures of superconductors (SCs) has experienced renewed interest due to the fact that they can be novel kinds of topological objects [1–19]. In this context, a line node in time-reversal (TR) invariant SCs is protected by a one-dimensional (1D) topological number and induces a Majorana flat band (MFB) on its surface[20–24]. These MFBs exhibit a zero-bias conductance peak that can be revealed through tunneling measurements in TR invariant SCs such as high-T_c cuprate SCs[25–31] and noncentrosymmetric SCs[32–34], and thus provide conclusive evidence for the existence of bulk topological line nodes.

In materials with strong spin-orbit interactions (SOIs), e.g., heavy fermion SCs, the formation of Cooper pairs is constrained by the underlying crystal structure because a group operation is followed by the spin operation[35,36]. When crystal symmetry forbids an irreducible representation (IR) of Cooper pairs in a highly symmetric subspace of the Brillouin zone (BZ), a symmetry-protected node arises[36–42]. Recently, there has been much effort devoted to exploring such symmetry-protected line nodes in SCs with (magnetic) non-symmorphic space group symmetry[43–48]; however, the corresponding physical phenomena remains unclear. Nevertheless, some of symmetry-protected line nodes are known to be simultaneously protected by a topological number[12,46], which implies the existence of MFBs.

In this paper, we unify the topology of symmetry-protected line nodes and MFBs. By taking general symmetry constraints affecting line nodes into account, we show that symmetry-protected line nodes host two different kinds of topological numbers: a 0D topological number that describes the topology of the symmetry-protected line nodes, and a 1D topological number that reflects the MFBs. The two topological numbers are intrinsically related to each other and the relationship between them fills the gap between the symmetry-protected line nodes and MFBs.

Our topological argument allows us to categorize line nodal SCs into three different classes with respect to the MFBs: (i) odd-parity SCs with TR or a magnetic translation symmetry, (ii) even-parity SCs with TR symmetry, and (iii) even-parity SCs with a magnetic translation symmetry. The three classes are directly linked to the symmetry-protected line nodes, as shown in Table I and II. Furthermore, we show that there is no MFB in Class (i) SCs , and that the magnetic translation is sensitive to the surface orientation, which provides an additional constraint on the MFBs in Class (iii) SCs. As a result, each case is distinguishable through surface sensitive measurements. Finally, we demonstrate the existence of a MFB in Class (iii) SCs based on a minimal model describing UPd_2Al_3, which hosts nodal loops on the Brillouin zone face (ZF). Interestingly, the MFB in this case only arises if the crystal symmetry protecting the nodal loops is broken, reflecting the additional constraint mentioned above.

IRs of Cooper pairs— First, we revisit the group theoretical results. In materials with strong SOIs, electron states respect symmetry of the crystal structure and are thus characterized by its IRs. Therefore, the possible formation of Cooper pairs is determined by the IRs of the electron states. For clarity, let $\gamma_{\boldsymbol{k}}(m)$ be an IR of the symmetry group $m \in G_{\boldsymbol{k}}$ for an electron with momentum $\boldsymbol{k}$, where $G_{\boldsymbol{k}}$ is the little group of $\boldsymbol{k}$. When electrons at $\boldsymbol{k}$ and $-\boldsymbol{k}$ form a Cooper pair, it can be represented by $P_{\boldsymbol{k}}(m) \equiv \gamma_{d\boldsymbol{k}}(m) \otimes \gamma_{\boldsymbol{k}}(m) - \gamma_{\boldsymbol{k}}(m) \otimes \gamma_{d\boldsymbol{k}}(m)$, where d is a symmetry operator satisfying $d\boldsymbol{k} = -\boldsymbol{k}$. Therefore, $P_{\boldsymbol{k}}$ is an induced representation in $G_{\boldsymbol{k}} + dG_{\boldsymbol{k}}$, and such anti-symmetrized IRs can be systematically calculated using the Herring's test[49,50] and the Mackey–Bradley theorem[51,52], $\chi[P_{\boldsymbol{k}}(m)] = \chi[\gamma_{\boldsymbol{k}}(m)]\chi[\gamma_{\boldsymbol{k}}(d^{-1}md)]$ and $\chi[P_{\boldsymbol{k}}(dm)] = -\chi[\gamma_{\boldsymbol{k}}(dmdm)]$, where χ is a character of the representation. In the following, we apply this theorem to the case of SCs with line nodes. In the case of a 3D BZ, a line node may occur along the intersection of a highly symmetric plane and the Fermi surface, so we must also take the mirror-reflection (MR) operation σ_h into account as crystal symmetry. If a Cooper pair lies on such a mirror plane, d then corresponds to either spatial inversion I, a two-fold rotation C_2, or TR θ. However, in order to take the non-symmorphic group symmetry into account, we must generalize the group operations

TABLE I. Character table of $P_{\boldsymbol{k}}$ and IR decompositions of $P_{\boldsymbol{k}}$ in the two possible mirror planes, $k_\perp = 0$ and $k_\perp = \pi$, where $\hat{\mathcal{E}}$ is the unit element of the crystal group symmetry and A_g, B_g, A_u, and B_u are IRs of C_{2h} generated by ($\hat{\mathcal{E}}$, $\hat{\mathcal{C}}_2$, $\hat{\mathcal{P}}$, $\hat{\mathcal{M}}$).

	$P_{k_\perp=0}$	$\hat{\mathcal{E}}$	$\hat{\mathcal{C}}_2$	$\hat{\mathcal{P}}$	$\hat{\mathcal{M}}$	Decomposition
(a-d)	$^\forall\boldsymbol{t}_\theta, \boldsymbol{t}_\sigma$	4	2	−2	0	$A_g + 2A_u + B_u$
	$P_{k_\perp=\pi}$	$\hat{\mathcal{E}}$	$\hat{\mathcal{C}}_2$	$\hat{\mathcal{P}}$	$\hat{\mathcal{M}}$	Decomposition
(a)	$[\boldsymbol{t}_\sigma]_\perp = [\boldsymbol{t}_\theta]_\perp = 0$	4	2	−2	0	$A_g + 2A_u + B_u$
(b)	$[\boldsymbol{t}_\sigma]_\perp \neq 0$, $[\boldsymbol{t}_\theta]_\perp = 0$	4	−2	−2	4	$A_g + 3B_u$
(c)	$[\boldsymbol{t}_\sigma]_\perp = 0$, $[\boldsymbol{t}_\theta]_\perp \neq 0$	4	2	−2	−4	$B_g + 3A_u$
(d)	$[\boldsymbol{t}_\sigma]_\perp \neq 0$, $[\boldsymbol{t}_\theta]_\perp \neq 0$	4	−2	−2	0	$B_g + A_u + 2B_u$

above so that $\hat{\mathcal{P}} = \{I|0\}$, $\hat{\mathcal{T}} = \{\theta|\boldsymbol{t}_\theta\}$, $\hat{\mathcal{M}} = \{\sigma_h|\boldsymbol{t}_\sigma\}$, and $\hat{\mathcal{C}}_2 = \hat{\mathcal{P}}\hat{\mathcal{M}}$, where the operator $\{p|\boldsymbol{a}\}$ acts on the position $\boldsymbol{r}$ as $\{p|\boldsymbol{a}\}\boldsymbol{r} = p\boldsymbol{r} + \boldsymbol{a}$, while $\boldsymbol{t}_\sigma$ and $\boldsymbol{t}_\theta$ correspond to the zero or half translation operators. We note that any non-symmorphic generalizations of I, θ, σ_h, and C_2 can be written in the above forms by an appropriate choice of the origin. Using the generalizations provided above, the operators $\hat{\mathcal{T}}$, $\hat{\mathcal{M}}$, and $\hat{\mathcal{C}}_2$ include magnetic translation, glide, and screw transformations, respectively, and thus allow for the complete classification of symmetry-protected line nodes.

The characters of $P_{\boldsymbol{k}}$ can thus be obtained using the Mackey–Bradley theorem, and are as listed in Table I[53], where $[\boldsymbol{t}_\sigma]_\perp$ and $[\boldsymbol{t}_\theta]_\perp$ correspond to translations perpendicular to the mirror plane. We find that the results can be classified into four different cases[46,48]: (a) $[\boldsymbol{t}_\sigma]_\perp = [\boldsymbol{t}_\theta]_\perp = 0$; (b) $[\boldsymbol{t}_\sigma]_\perp \neq 0$ and $[\boldsymbol{t}_\theta]_\perp = 0$; (c) $[\boldsymbol{t}_\sigma]_\perp = 0$ and $[\boldsymbol{t}_\theta]_\perp \neq 0$; and (d) $[\boldsymbol{t}_\sigma]_\perp \neq 0$ and $[\boldsymbol{t}_\theta]_\perp \neq 0$. In the basal plane (BP) ($k_\perp = 0$, where $k_\perp$ is the momentum normal to the mirror plane), the symmetry operators have the common expected characters in all cases, but on the ZF ($k_\perp = \pi$), the characters in each case are different. Comparing these characters with those of the IRs of C_{2h}, we can thus obtain the IR decomposition of $P_{\boldsymbol{k}}$, which is summarized in Table I and indicates the possible pairing symmetries of Cooper pairs that are consistent with the crystal structure.

Topology of symmetry-protected line nodes—Let us now discuss the symmetry-protected line nodes from the viewpoint of topology. Such topological properties are of importance in identifying the bulk–boundary correspondence, i.e., the line-node-induced MFBs. We can formulate the topology of line nodes using the Bogoliubov–de Gennes (BdG) Hamiltonian, $H_{\rm BdG} = \frac{1}{2}\sum_{\boldsymbol{k},\alpha,\beta} \Psi^\dagger_{\boldsymbol{k},\alpha}\tilde{H}(\boldsymbol{k})_{\alpha\beta}\Psi_{\boldsymbol{k},\beta}$, with $\Psi^T_{\boldsymbol{k},\alpha} = (c_{\boldsymbol{k},\alpha}, c^\dagger_{-\boldsymbol{k},\alpha})$. We note that this Hamiltonian exhibits particle-hole (PH) symmetry i.e. $C\tilde{H}(\boldsymbol{k})C^\dagger = -\tilde{H}(-\boldsymbol{k})$, where $C = \tau_x K$ is the anti-unitary operator, $\boldsymbol{\tau}$ is the Pauli matrix in Nambu space, and K is the complex conjugate. We choose a periodic Bloch basis so that $\tilde{H}(\boldsymbol{k}) = \tilde{H}(\boldsymbol{k}+\boldsymbol{G})$, where $\boldsymbol{G}$ a reciprocal lattice (RL) vector.

First, we consider how the symmetry operations affect the BdG Hamiltonian. The creation operator of an electron satisfies $\{p|\boldsymbol{a}_p\}c^\dagger_{\boldsymbol{k},\alpha}\{p|\boldsymbol{a}_p\}^{-1} = c^\dagger_{p\boldsymbol{k},\beta}[e^{-ip\boldsymbol{k}\cdot\boldsymbol{a}_p}U(p)_{\boldsymbol{k}}]_{\beta\alpha}$, where $\{p|\boldsymbol{a}_p\} = \hat{\mathcal{P}}$, $\hat{\mathcal{M}}$, or $\hat{\mathcal{C}}_2$. If the BdG Hamiltonian is invariant with respect to the symmetry operations, one yields $\tilde{U}(p)_{\boldsymbol{k}}\tilde{H}(\boldsymbol{k})\tilde{U}(p)^\dagger_{\boldsymbol{k}} = \tilde{H}(p\boldsymbol{k})$ with $\tilde{U}(p)_{\boldsymbol{k}} = \mathrm{diag}[U(p)_{\boldsymbol{k}}, \eta_p U(p)^*_{-\boldsymbol{k}}]$. Here, $\eta_p = \pm 1$, where the choice of sign is the same as the sign of the character of p in the IR of $\Delta(\boldsymbol{k})$. In addition, $\hat{\mathcal{T}}$ acts on the creation operators in a similar way to TR symmetry, and is thus accompanied by an additional momentum factor for $\boldsymbol{t}_\theta \neq 0$, i.e., $\hat{\mathcal{T}}c^\dagger_{\boldsymbol{k},\alpha}\hat{\mathcal{T}}^{-1} = c^\dagger_{-\boldsymbol{k},\beta}[e^{i\boldsymbol{k}\cdot\boldsymbol{t}_\theta}U(\theta)_{\boldsymbol{k}}]_{\beta\alpha}$, which yields $\tilde{U}(\theta)_{\boldsymbol{k}}\tilde{H}(\boldsymbol{k})^*\tilde{U}(\theta)^\dagger_{\boldsymbol{k}} = \tilde{H}(-\boldsymbol{k})$, with $\tilde{U}(\theta)_{\boldsymbol{k}} = \mathrm{diag}[U(\theta)_{\boldsymbol{k}}, U(\theta)^*_{-\boldsymbol{k}}]$.

TABLE II. (Color online) Topology of the symmetry-protected line nodes, labeled by the symbol $M^{p\,q}_{g(u)}$. The superscripts p, q are defined by $p = e^{-i\boldsymbol{G}_\sigma\cdot\boldsymbol{t}_\sigma}\eta_{\sigma_h}$ and $q = e^{-i\boldsymbol{G}_\sigma\cdot\boldsymbol{t}_\theta}\eta_{\sigma_h}$, respectively, while the subscript $g(u)$ indicates whether the SC has even (g) or odd (u) parity. The bottom table shows the comparison between Table I and the 0D topological numbers, where $A_g(B_u)$ and $B_g(A_u)$ in the BP correspond to the $M^{++}_{g(u)}$ and $M^{--}_{g(u)}$ classes, respectively. The labels (i)–(iii) indicate the SC class of MFBs.

Topo. #	M_g^{++}	M_g^{+-}	M_g^{-+}	M_g^{--}	M_u^{++}	M_u^{+-}	M_u^{-+}	M_u^{--}
0D	0	$2\mathbb{Z}$	0	$\mathbb{Z}_2$	0	$2\mathbb{Z}$	0	0
1D	$2\mathbb{Z}$	$2\mathbb{Z}$	$2\mathbb{Z}$	$2\mathbb{Z}$	0	0	0	0

	A_g		B_g		A_u		B_u	
Cases	BP	ZF	BP	ZF	BP	ZF	BP	ZF
(a)	0	0	(ii) $\mathbb{Z}_2$	$\mathbb{Z}_2$	0	0	0	0
(b)	0	0	(ii) $\mathbb{Z}_2$	$2\mathbb{Z}$	(i) 0	$2\mathbb{Z}$	0	0
(c)	(iii) 0	$2\mathbb{Z}$	(iii) $\mathbb{Z}_2$	0	0	0	(i) 0	$2\mathbb{Z}$
(d)	(iii) 0	$\mathbb{Z}_2$	(iii) $\mathbb{Z}_2$	0	0	0	0	0

Next, we clarify the relations between the symmetry operations. On the mirror plane, the PH operator satisfies $C\tilde{U}(p)_{\boldsymbol{k}} = \eta_p\tilde{U}(p)_{-\boldsymbol{k}}C$, while $U(\sigma_h)_{\boldsymbol{k}}$, $U(I)_{\boldsymbol{k}}$, and $U(\theta)_{\boldsymbol{k}}$ satisfy $U(I)_{\boldsymbol{k}}U(\sigma_h)_{\boldsymbol{k}} = \eta_{I,\sigma_h}U(\sigma_h)_{-\boldsymbol{k}}U(I)_{\boldsymbol{k}}$ and $U(\theta)_{\boldsymbol{k}}U(\sigma_h)^*_{\boldsymbol{k}} = \eta_{\theta,\sigma_h}e^{i(\sigma_h\boldsymbol{k}-\boldsymbol{k})\cdot\boldsymbol{t}_\theta}U(\sigma_h)_{-\boldsymbol{k}}U(\theta)_{\boldsymbol{k}}$, where we have used $U(pp')_{\boldsymbol{k}} = \eta_{p,p'}U(p'p)_{\boldsymbol{k}}$ and the additional phase factor $e^{i(\sigma_h\boldsymbol{k}-\boldsymbol{k})\cdot\boldsymbol{t}_\theta}$ (called the factor system[52]) is only nontrivial on the ZF. Hereafter, we assume $\eta_{I,\sigma_h} = \eta_{\theta,\sigma_h} = 1$ as all space groups do.

A line node in superconducting gaps, in general, appears either at a) a general position or b) on a high-symmetric plane, i.e., a mirror or a glide plane since it occurs on the Fermi surface. See Fig. 1 (a). For the former case, symmetries affecting a line node are ones keeping the arbitrary position of line node. Such symmetry operations are given by the PH-like operator $\mathcal{C}_{\boldsymbol{k}} \equiv C\tilde{U}(I)_{\boldsymbol{k}}$, the TR-like operator $\mathcal{T}_{\boldsymbol{k}} \equiv \tilde{U}(I)_{-\boldsymbol{k}}\tilde{U}(\theta)_{\boldsymbol{k}}K$, which are obtained from combinations of the PH and TR operators with inversion operators, and the chiral operator $\Gamma_{\boldsymbol{k}} \equiv iC\tilde{U}(\theta)_{\boldsymbol{k}}K$. Here, $\eta_I\mathcal{C}^2_{\boldsymbol{k}} = -\mathcal{T}^2_{\boldsymbol{k}} = \Gamma^2_{\boldsymbol{k}} = 1$. On

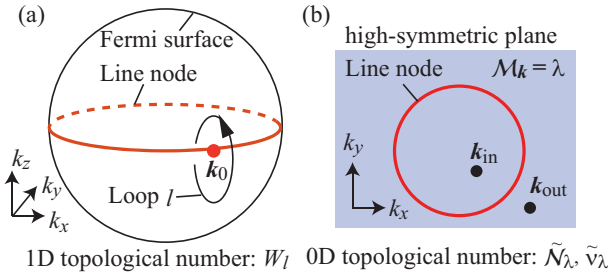

FIG. 1. (Color online) When a line node appears at a general position $\boldsymbol{k}_0$, it is encircled by a loop l (a). On the other hand, if one lies on a high-symmetric plane, two points $\boldsymbol{k}_{\rm in}$ and $\boldsymbol{k}_{\rm out}$ encircle it (b).

the other hand, for the latter case, a line node is on a high-symmetric plane, which may be enforced by the MR operation $\tilde{U}(\sigma)_{\boldsymbol{k}}$. Since $\tilde{U}(\sigma)_{\boldsymbol{k}}^2 = -e^{-i\boldsymbol{G}_\sigma\cdot\boldsymbol{t}_\sigma}$, the sign of the squared operator may also change at the ZF. We conveniently fix the sign by defining $\mathcal{M}_{\boldsymbol{k}} \equiv e^{i\boldsymbol{G}_\sigma\cdot\boldsymbol{t}_\sigma/2}\tilde{U}(\sigma)_{\boldsymbol{k}}$ which satisfies $\mathcal{M}_{\boldsymbol{k}}^2 = -1$, where $\boldsymbol{G}_\sigma$ is the RL vector normal to the high-symmetric plane. Using the above relationships, we then obtain the commutation relations:

$$\mathcal{C}_{\boldsymbol{k}}\mathcal{M}_{\boldsymbol{k}} = e^{-i\boldsymbol{G}_\sigma\cdot\boldsymbol{t}_\sigma}\,\eta_{\sigma_h}\mathcal{M}_{\boldsymbol{k}}\mathcal{C}_{\boldsymbol{k}}, \tag{1a}$$

$$\Gamma_{\boldsymbol{k}}\mathcal{M}_{\boldsymbol{k}} = e^{-i\boldsymbol{G}_\sigma\cdot\boldsymbol{t}_\theta}\,\eta_{\sigma_h}\mathcal{M}_{\boldsymbol{k}}\Gamma_{\boldsymbol{k}}, \tag{1b}$$

while the commutation relation between $\mathcal{T}_{\boldsymbol{k}}$ and $\mathcal{M}_{\boldsymbol{k}}$ can be determined from Eq. (1). Since $\boldsymbol{G}_\sigma\cdot\boldsymbol{t}_p = 2\pi[\boldsymbol{t}_p]_\perp$, the right-hand side of Eq. (1) may change sign in the BP and the ZF, depending on the action of $[\boldsymbol{t}_\sigma]_\perp$ and $[\boldsymbol{t}_\theta]_\perp$.

a) line node at a general position: As a vortex in the momentum space, stability of a line node is ensured by a 1D topological number defined on a circle enclosing the line node. However, the PH-like or TR-like operator does not give non-zero 1D topological number, so the chiral symmetry is required[9,16,19,54]. Furthermore, since $\mathcal{C}_{\boldsymbol{k}}^2 = \eta_I$, even-parity SCs ($\eta_I = 1$) and odd-parity SCs ($\eta_I = -1$) belong to different Altland–Zirnbauer (AZ) classes[55,56], and only even-parity SCs can support a non-zero 1D topological number[9]. For even-parity SCs, the 1D topological number in terms of $\Gamma_{\boldsymbol{k}}$ can be defined on a loop l:

$$W_l = \frac{i}{4\pi}\oint_l d\boldsymbol{k}\cdot\mathrm{Tr}\left[\Gamma_{\boldsymbol{k}}\tilde{H}(\boldsymbol{k})^{-1}\boldsymbol{\partial}_{\boldsymbol{k}}\tilde{H}(\boldsymbol{k})\right]. \tag{2}$$

b) line node on a high-symmetric plane: We take $\mathcal{M}_{\boldsymbol{k}}$ into account as a symmetry operation relevant to a line node in addition to $\mathcal{C}_{\boldsymbol{k}}$, $\mathcal{T}_{\boldsymbol{k}}$, and $\Gamma_{\boldsymbol{k}}$. On a high-symmetric plane, a line node separates the 2D BZ into two disjoint regions, which are distinguished by a 0D topological number. See Fig. 1 (b). For a 0D topological number, we refer to the topological periodic table presented in[57–62] and regarding $\mathcal{T}_{\boldsymbol{k}}$, $\mathcal{C}_{\boldsymbol{k}}$, and $\Gamma_{\boldsymbol{k}}$ in terms of the AZ symmetry.

On the mirror plane, the MR operator commutes with the BdG Hamiltonian and so the BdG Hamiltonian splits into MR sectors: $\tilde{H} \to \tilde{h}_\lambda \oplus \tilde{h}_{-\lambda}$, where λ is an eigenvalue of $\mathcal{M}_{\boldsymbol{k}}$. Then, $\Gamma_{\boldsymbol{k}}$ ($\mathcal{C}_{\boldsymbol{k}}$ and $\mathcal{T}_{\boldsymbol{k}}$) exists within the MR sectors if it (anti-)commutes with $\mathcal{M}_{\boldsymbol{k}}$. For instance, when $[\mathcal{C}_{\boldsymbol{k}}, \mathcal{M}_{\boldsymbol{k}}] = \{\mathcal{T}_{\boldsymbol{k}}, \mathcal{M}_{\boldsymbol{k}}\} = \{\Gamma_{\boldsymbol{k}}, \mathcal{M}_{\boldsymbol{k}}\} = 0$, the symmetry class of each MR sector is the AII class ($\mathcal{T}_{\boldsymbol{k}}^2 = -1$) and its 0D topological number is $2\mathbb{Z}$. As such, we have determined the possible 0D topological numbers in the MR sectors and summarized them in Table II. The obtained 0D topological numbers $2\mathbb{Z}$ and $\mathbb{Z}_2$ of a line node in the MR sector h_λ can then be defined as

$$\tilde{\mathcal{N}}_\lambda = \tilde{n}(\boldsymbol{k}_{\rm out})_\lambda - \tilde{n}(\boldsymbol{k}_{\rm in})_\lambda, \tag{3}$$

$$(-1)^{\tilde{\nu}_\lambda} = \mathrm{sgn}\left[\frac{\mathrm{Pf}\{\tilde{h}_\lambda(\boldsymbol{k}_{\rm out})L_{\boldsymbol{k}_{\rm out},\lambda}\}}{\mathrm{Pf}\{\tilde{h}_\lambda(\boldsymbol{k}_{\rm in})L_{\boldsymbol{k}_{\rm in},\lambda}\}}\right], \tag{4}$$

respectively, where $\tilde{n}(\boldsymbol{k})_\lambda$ is the number of occupied states with momentum $\boldsymbol{k}$, $\mathcal{C}_{\boldsymbol{k}} = (L_{\boldsymbol{k},\lambda} \oplus L_{\boldsymbol{k},-\lambda})K$, and $\boldsymbol{k}_{\rm in(out)}$ is the momentum inside (outside) the line node. In the weak coupling limit, i.e., $\Delta(\boldsymbol{k}) \to 0$, Eqs. (3) and (4) are directly linked to the Fermi surface topology: If we define $\mathcal{N}_\lambda = n(\boldsymbol{k}_{\rm out})_\lambda - n(\boldsymbol{k}_{\rm in})_\lambda$ in the normal Hamiltonian to be the topological number of the Fermi surface in the mirror sector with eigenvalue λ, Eqs. (3) and (4) are reduced to $\tilde{\mathcal{N}}_\lambda = 2\mathcal{N}_\lambda$ and $(-1)^{\tilde{\nu}_\lambda} = (-1)^{\mathcal{N}_\lambda}$[53], which implies that a nodal loop is only topologically stable if $\mathcal{N}_\lambda \neq 0$.

We are now in a position to elucidate the relationship between the group theoretical and topological classifications. The IRs A_g, A_u, B_g, and B_u then correspond to the topological classifications labeled by M_g^{++}, M_u^{--}, M_g^{--}, and M_u^{++} in the BP, where the superscripts of the symbol encode the commutation relations (1a) and (1b) and the subscript indicates even (g) or odd (u) parity. Moreover, the MR symmetry classes in the ZF depend on $[\boldsymbol{t}_\sigma]_\perp$ and $[\boldsymbol{t}_\theta]_\perp$ due to Eq. (1). In Table II, we have summarized the correspondence between the 0D topological numbers and the four cases, (a)–(d). In comparison to Tables I and II, we find a one-to-one correspondence, in which the absence of IRs coincides with the presence of the 0D topological numbers.

Possible MFBs—Finally, we consider the connection between symmetry-protected line nodes and MFBs, which are characterized by 0D and 1D topological numbers, respectively. As was discussed above, the 1D topological number exists only for even-parity SCs, so does MFBs. In such even-parity SCs, the 1D and 0D topological numbers are intrinsically related to each other and satisfy[53]

$$|\tilde{\mathcal{N}}_\lambda| = |W_l|, \quad (-1)^{\tilde{\nu}_\lambda} = (-1)^{\frac{W_l}{2}}, \tag{5}$$

which implies that a symmetry-protected line node is always accompanied by the 1D topological number. We note also that the 1D topological number survives even when the MR symmetry is broken, which reflects the strong stability of the line nodes.

Using Table II and Eq. (5), we can identify three classes with respect to the stability of the line nodes. A line node may be protected by: (i) the 0D topological number in odd-parity SCs with TR or a magnetic translation symmetry, or alternatively, by both the 0D and 1D topological numbers in even parity SCs with (ii) TR or (iii) a magnetic translation symmetry. We immediately find that there is no MFB in Class (i) SCs since there is no 1D topological number corresponding to an MFB in odd-parity SCs. In order to demonstrate the existence of MFBs in Class (ii) and (iii) SCs, consider a system with an open boundary, e.g., the $x_i = 0$ plane. Then, an MFB appears on the $x_i = 0$ plane if the 1D topological number (2) defined on the loop $l(k_j, k_l) = \{(k_i, k_j, k_l) | -\pi \leq k_i \leq \pi\}$ is nonzero[20,63], where (k_i, k_j, k_l) are perpendicular to each other, and $l(k_j, k_l)$ does not intersect with the line node. For SCs satisfying the conditions of Class (ii), the operator $\hat{\mathcal{T}}$ corresponds to a pure TRS, so $l(k_j, k_l)$ can be defined for arbitrary surface direction. Thus, an MFB appears on the SC's surface in analogy with high-T_c cuprate SCs[64,65]. On the other hand, $\hat{\mathcal{T}}$ in Class (iii) corresponds to a magnetic translation, so $l(k_j, k_l)$ needs to be compatible with a translation vector $\boldsymbol{t}_\theta$, i.e., an MFB only arises when one satisfies $\boldsymbol{t}_\theta \cdot \hat{\boldsymbol{e}}_i = 0$ for Class (iii) SCs, where $\hat{\boldsymbol{e}}_i$ is a unit vector normal to the surface. Note that the behavior we have outlined here is similar to that of surface states in aniferromagnetic topological insulators[66–73]. Thus, a limitation on possible MFBs in Class (iii) SCs appears in contrast to MFBs in Class (ii) and non-centrosymmetric SCs[32–34]. In particular, when $\boldsymbol{t}_\theta$ is perpendicular to the mirror plane, MFBs do not exist on any surface because no surface direction simultaneously satisfies the constraints arising from the magnet translation and the MR symmetry. Thus, a distortion or interaction that breaks the MR symmetry is necessary to reveal the hidden MFBs.

Application to UPd_2Al_3—In order to verify the existence of a MFB in Class (iii) SCs, let us consider a minimal model of the antiferromagnetic SC UPd_2Al_3[45]. The antiferromagnetic phase of this material is specified by the magnetic space group P_b2_1/m, and the two U atoms are situated at the $(0,0,0)$ and $(0,0,\frac{1}{2})$ positions in the magnetic unit cell. Taking a single orbital at each U site into account, the tight-binding model can then be given by $H(\boldsymbol{k}) = \epsilon(\boldsymbol{k})_1 + \epsilon(\boldsymbol{k})_2\sigma_x(k_z) + \delta_M\sigma_z s_x$, where $\epsilon(\boldsymbol{k})_1 = -2t_{xy}(\cos k_x + \cos k_y) - 2t'_z \cos k_z$, $\epsilon(\boldsymbol{k})_2 = -2t_z \cos\frac{k_z}{2}$, and $\sigma_x(k_z) \equiv \cos\frac{k_z}{2}\sigma_x + \sin\frac{k_z}{2}\sigma_y$. The constants t_{xy}, t'_z, and t_z are hopping parameters and δ_M represents the molecular field in terms of the magnetic moment . For simplicity, the gap function is assumed to be given by the s-wave spin-singlet pairing, $\Delta_0 i s_y$, and the symmetry operators are then given by $\mathcal{C}_{\boldsymbol{k}} = e^{i\frac{k_z}{2}}(\cos\frac{k_z}{2}\sigma_0 - i\sin\frac{k_z}{2}\sigma_z)\tau_x K$, $\mathcal{T}_{\boldsymbol{k}} = e^{i\frac{k_z}{2}} i\sigma_x s_y K$, $\Gamma_{\boldsymbol{k}} = -\sigma_x(k_z)s_y\tau_x$, and $\mathcal{M}_{\boldsymbol{k}} = i\sigma_x s_z \tau_z$, where $\boldsymbol{\sigma}$ and $\boldsymbol{s}$ are the Pauli matrices in the sublattice and spin spaces, respectively. This model is known to host two nodal loops in the $k_z = \pi$ plane[45]. Since the MR symmetry class is M_g^{--}, the nodal loops are protected by both 0D and 1D topological numbers. In fact, using Eq. (5), we find $\nu_\lambda = 1$ and $|W_l| = 2$ for each nodal loop and the resulting nontrivial Fermi surface topology is shown in Fig. 2(a)[53]. Notably, MFBs are absent in all surface planes because $\boldsymbol{t}_\theta = \frac{1}{2}\hat{\boldsymbol{e}}_z$ is perpendicular to the mirror plane.

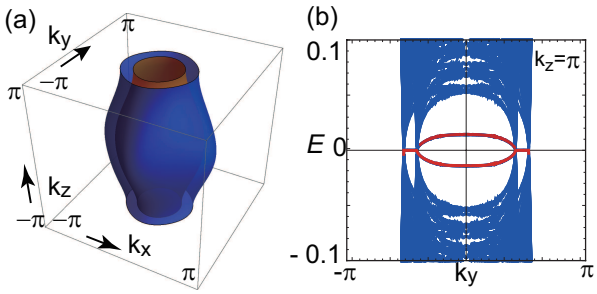

FIG. 2. (Color online) (a) Fermi surface of our model. (b) Energy spectrum on the (100) plane, where the thick red line indicates the surface state.

However, when we add an MR-breaking distortion term, e.g., $2t_{xz}\sin k_x \sin\frac{k_z}{2}\sigma_x(k_z)$ to the Hamiltonian, the nodal loop escapes from the mirror plane. In this case, the surface state can be numerically determined and the MFBs are revealed by the MR-breaking distortion, as shown in Fig. 2(b).

Concluding remarks– We have established the relationship between symmetry-protected line nodes and MFBs. Classes (i)-(iii) of the symmetry-protected line nodes provide a comprehensive classification of line-node-induced MFBs on unconventional SCs, where noncentrosymmetric SCs with line nodes are included in Class (ii) SCs as its stability is ensured by the pure TR operator. It is straightforward to generalize our results to higher-symmetric cases by relating IRs in C_{2h} and compatible ones. Based on our theory connecting the group theory and topological arguments, various line-nodal SCs are categorized. For instance, UPt_3[43] is classified into the Class (i) and UPd_2Al_3[45] and Sr_2IrO_4 ($-++-$ state)[47] are the Class (iii), while ordinary d-wave SCs such as high-T_c cuprates and heavy fermion $CeCoIn_5$ are categorized to the Class (ii). These SCs are distinguished by MFBs which can be detected through surface sensitive experiments such as tunneling conductance measurements.

The authors are grateful to T. Nomoto and A. Yamakage for useful discussions. This work was supported by the Grants-in-Aid for Scientific Research on Innovative Areas "J-Physics" (Grant No. JP15H05884) and "Topological Material Science" (Grant Nos. JP15H05855 and JP16H00991) from JSPS of Japan, and by JSPS KAKENHI Grant Nos. 15K05164, JP15H05745, JP16H06861, JP17H02922, and JP17J09908. S.K. was supported by a CREST project (JPMJCR16F2) from Japan Science and Technology Agency (JST), and the Building of Consortia for the Development of Human Resources in Science and Technology.

[1] G. E. Volovik, *The Universe in a Helium Droplet* (Oxford University Press, Oxford, 1972).
[2] P. Hořava, Phys. Rev. Lett. **95**, 016405 (2005).
[3] M. Sato, Phys. Rev. B **73**, 214502 (2006).
[4] B. Béri, Phys. Rev. B **81**, 134515 (2010).
[5] Y. X. Zhao and Z. D. Wang, Phys. Rev. Lett. **110**, 240404 (2013).
[6] K. Shiozaki and M. Sato, Phys. Rev. B **90**, 165114 (2014).
[7] S. A. Yang, H. Pan, and F. Zhang, Phys. Rev. Lett. **113**, 046401 (2014).
[8] C.-K. Chiu and A. P. Schnyder, Phys. Rev. B **90**, 205136 (2014).
[9] S. Kobayashi, K. Shiozaki, Y. Tanaka, and M. Sato, Phys. Rev. B **90**, 024516 (2014).
[10] T. Morimoto and A. Furusaki, Phys. Rev. B **89**, 235127 (2014).
[11] P. Goswami and A. H. Nevidomskyy, Phys. Rev. B **92**, 214504 (2015).
[12] S. Kobayashi, Y. Yanase, and M. Sato, Phys. Rev. B **94**, 134512 (2016).
[13] D. F. Agterberg, P. M. R. Brydon, and C. Timm, Phys. Rev. Lett. **118**, 127001 (2017).
[14] M. Sato and S. Fujimoto, Journal of the Physical Society of Japan **85**, 072001 (2016).
[15] T. Mizushima, Y. Tsutsumi, T. Kawakami, M. Sato, M. Ichioka, and K. Machida, Journal of the Physical Society of Japan **85**, 022001 (2016).
[16] Y. X. Zhao, A. P. Schnyder, and Z. D. Wang, Phys. Rev. Lett. **116**, 156402 (2016).
[17] C.-K. Chiu, J. C. Y. Teo, A. P. Schnyder, and S. Ryu, Rev. Mod. Phys. **88**, 035005 (2016).
[18] M. Sato and Y. Ando, Reports on Progress in Physics **80**, 076501 (2017).
[19] T. Bzdušek and M. Sigrist, Phys. Rev. B **96**, 155105 (2017).
[20] M. Sato, Y. Tanaka, K. Yada, and T. Yokoyama, Phys. Rev. B **83**, 224511 (2011).
[21] A. P. Schnyder and S. Ryu, Phys. Rev. B **84**, 060504 (2011).
[22] S. Matsuura, P.-Y. Chang, A. P. Schnyder, and S. Ryu, New Journal of Physics **15**, 065001 (2013).
[23] A. P. Schnyder and P. M. R. Brydon, Journal of Physics: Condensed Matter **27**, 243201 (2015).
[24] MFBs exist even in line-nodal SCs without TR symmetry, but they are not as stable as that in SCs with TR symmetry[74].
[25] Y. Tanaka and S. Kashiwaya, Phys. Rev. Lett. **74**, 3451 (1995).
[26] L. Alff, H. Takashima, S. Kashiwaya, N. Terada, H. Ihara, Y. Tanaka, M. Koyanagi, and K. Kajimura, Phys. Rev. B **55**, R14757 (1997).
[27] T. Löfwander, V. S. Shumeiko, and G. Wendin, Superconductor Science and Technology **14**, R53 (2001).
[28] J. Y. T. Wei, N.-C. Yeh, D. F. Garrigus, and M. Strasik, Phys. Rev. Lett. **81**, 2542 (1998).
[29] I. Iguchi, W. Wang, M. Yamazaki, Y. Tanaka, and S. Kashiwaya, Phys. Rev. B **62**, R6131 (2000).
[30] A. Biswas, P. Fournier, M. M. Qazilbash, V. N. Smolyaninova, H. Balci, and R. L. Greene, Phys. Rev. Lett. **88**, 207004 (2002).
[31] B. Chesca, H. J. H. Smilde, and H. Hilgenkamp, Phys. Rev. B **77**, 184510 (2008).
[32] P. M. R. Brydon, A. P. Schnyder, and C. Timm, Phys. Rev. B **84**, 020501 (2011).
[33] K. Yada, M. Sato, Y. Tanaka, and T. Yokoyama, Phys. Rev. B **83**, 064505 (2011).
[34] A. P. Schnyder, P. M. R. Brydon, and C. Timm, Phys. Rev. B **85**, 024522 (2012).
[35] P. W. Anderson, Phys. Rev. B **30**, 4000 (1984).
[36] M. Sigrist and K. Ueda, Rev. Mod. Phys. **63**, 239 (1991).
[37] E. I. Blount, Phys. Rev. B **32**, 2935 (1985).
[38] G. E. Volovik and L. P. Gor'kov, JETP Lett. **39**, 674 (1984).
[39] G. E. Volovik and L. P. Gor'kov, Sov. Phys. JETP **61**, 843 (1984).
[40] K. Ueda and T. M. Rice, Phys. Rev. B **31**, 7114 (1985).
[41] V. G. Yarzhemsky and E. N. Murav'ev, Journal of Physics: Condensed Matter **4**, 3525 (1992).
[42] V. G. Yarzhemsky, physica status solidi (b) **209**, 101 (1998).
[43] T. Micklitz and M. R. Norman, Phys. Rev. B **80**, 100506 (2009).
[44] T. Micklitz and M. R. Norman, Phys. Rev. B **95**, 024508 (2017).
[45] T. Nomoto and H. Ikeda, Journal of the Physical Society of Japan **86**, 023703 (2017).
[46] T. Micklitz and M. R. Norman, Phys. Rev. Lett. **118**, 207001 (2017).
[47] S. Sumita, T. Nomoto, and Y. Yanase, Phys. Rev. Lett. **119**, 027001 (2017).
[48] S. Sumita and Y. Yanase, ArXiv e-prints (2018), arXiv:1801.03293 [cond-mat.supr-con].
[49] C. Herring, Phys. Rev. **52**, 361 (1937).
[50] E. P. Wigner, *Group Theory and its Application to the Quantum Mechanics of Atomic Spectra* (Academic Press, New York, 1959).
[51] C. J. Bradley and B. L. Davies, Journal of Mathematical Physics **11**, 1536 (1970).
[52] C. J. Bradley and A. P. Cracknell, *The Mathematical Theory of Symmetry in Solids* (Oxford University Press, New York, 2003).
[53] See the Supplemental Material at [URL will be inserted by publisher] for the detail calculation.
[54] PT symmetry also enables us to define the 1D $\mathbb{Z}_2$ number, but in the case of superconductors, either P or T should be preserved in order for electrons at $\boldsymbol{k}$ and $-\boldsymbol{k}$ to form a bulk Cooper pair. Thus, PT symmetry implies the presence of T, which gives chiral symmetry with PH symmetry. The $\mathbb{Z}_2$ number then reduces to the parity of Eq. (2).
[55] M. R. Zirnbauer, Journal of Mathematical Physics **37**, 4986 (1996).
[56] A. Altland and M. R. Zirnbauer, Phys. Rev. B **55**, 1142 (1997).
[57] A. P. Schnyder, S. Ryu, A. Furusaki, and A. W. W. Ludwig, Phys. Rev. B **78**, 195125 (2008).
[58] A. P. Schnyder, S. Ryu, A. Furusaki, and A. W. W. Ludwig, AIP Conference Proceedings **1134**, 10 (2009).
[59] A. Kitaev, AIP Conference Proceedings **1134**, 22 (2009).
[60] S. Ryu, A. P. Schnyder, A. Furusaki, and A. W. W. Ludwig, New Journal of Physics **12**, 065010 (2010).
[61] C.-K. Chiu, H. Yao, and S. Ryu, Phys. Rev. B **88**, 075142 (2013).
[62] T. Morimoto and A. Furusaki, Phys. Rev. B **88**, 125129

(2013).
[63] S. Ryu and Y. Hatsugai, Phys. Rev. Lett. **89**, 077002 (2002).
[64] Y. Tanaka, Y. Mizuno, T. Yokoyama, K. Yada, and M. Sato, Phys. Rev. Lett. **105**, 097002 (2010).
[65] Y. Tanaka, M. Sato, and N. Nagaosa, Journal of the Physical Society of Japan **81**, 011013 (2012).
[66] R. S. K. Mong, A. M. Essin, and J. E. Moore, Phys. Rev. B **81**, 245209 (2010).
[67] A. M. Turner, Y. Zhang, R. S. K. Mong, and A. Vishwanath, Phys. Rev. B **85**, 165120 (2012).
[68] A. M. Essin and V. Gurarie, Phys. Rev. B **85**, 195116 (2012).
[69] S. Miyakoshi and Y. Ohta, Phys. Rev. B **87**, 195133 (2013).
[70] T. Yoshida, R. Peters, S. Fujimoto, and N. Kawakami, Phys. Rev. B **87**, 085134 (2013).
[71] P. Baireuther, J. M. Edge, I. C. Fulga, C. W. J. Beenakker, and J. Tworzydło, Phys. Rev. B **89**, 035410 (2014).
[72] R.-X. Zhang and C.-X. Liu, Phys. Rev. B **91**, 115317 (2015).
[73] F. Bègue, P. Pujol, and R. Ramazashvili, Physics Letters A **381**, 1268 (2017).
[74] S. Kobayashi, Y. Tanaka, and M. Sato, Phys. Rev. B **92**, 214514 (2015).